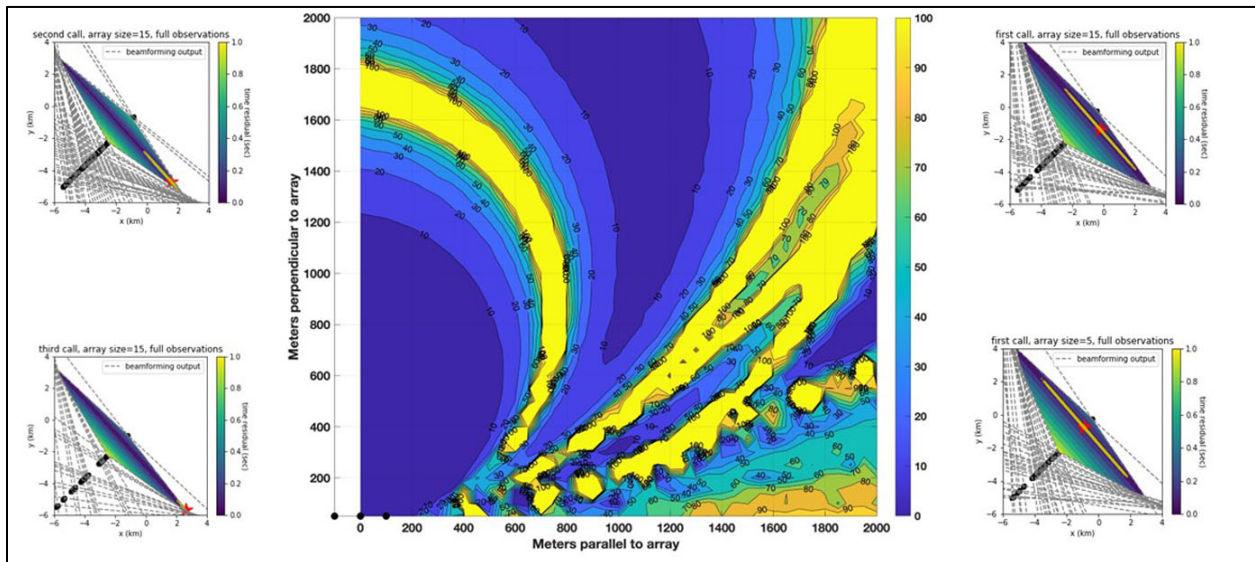# Optimization of Towed Passive Acoustic Monitoring (PAM) Array Design and Performance Study (Passive Acoustic Monitoring Study)

BOEM
Bureau of Ocean Energy
Management

# Optimization of Towed Passive Acoustic Monitoring (PAM) Array Design and Performance Study (Passive Acoustic Monitoring Study)

February 2021

Authors:
Aaron Thode
Shima Abadi
Mary Jo Barkaszi

**US Department of the Interior**
**Bureau of Ocean Energy Management**
**Sterling, VA**

BOEM
Bureau of Ocean Energy
Management

# DISCLAIMER

Study concept, oversight, and funding were provided by the US Department of the Interior, Bureau of Ocean Energy Management (BOEM), Environmental Studies Program, Washington, DC, under Contract Number 140M0119F0051. This report has been technically reviewed by BOEM, and it has been approved for publication. The views and conclusions contained in this document are those of the authors and should not be interpreted as representing the opinions or policies of the US Government, nor does mention of trade names or commercial products constitute endorsement or recommendation for use.

# REPORT AVAILABILITY

To download a PDF file of this report, go to the US Department of the Interior, Bureau of Ocean Energy Management Data and Information Systems webpage (http://www.boem.gov/Environmental-Studies-EnvData/), click on the link for the Environmental Studies Program Information System (ESPIS), and search on 2021-086. The report is also available at the National Technical Reports Library at https://ntrl.ntis.gov/NTRL/.

# CITATION

Thode A, Abadie S, Barkaszi MJ. 2021. Optimization of Towed Passive Acoustic Monitoring (PAM) Array Design and Performance Study (Passive Acoustic Monitoring Study). Sterling (VA): US Department of the Interior, Bureau of Ocean Energy Management. OCS Study BOEM 2021-086. 32 p.

# ABOUT THE COVER

Graphic images provided by A. Thode and S. Abadie.

# Executive Summary

A numerical model for simulating the localization performance of a three- or four-hydrophone towed passive acoustic monitoring (PAM) array on multiple species clusters was developed that allows the Bureau of Ocean Energy Management (BOEM) to assess the localization efficacy of towed PAM arrays proposed in mitigation and monitoring plans for offshore wind farm development and other operations. Simulations of a 200-m aperture array were run for three marine mammal signal types of interest: sperm whale, right whale, and beaked whale. The ability to localize a marine mammal call using PAM systems commonly deployed for mitigation surveys conducted in support of offshore wind farm development requires several conditions and assumptions. In order to localize, the call must first be detected. A detection's range will be dictated by the received amplitude of the signal, which in turn depends on the species, distance, and relative orientation to the receiver, as well as the noise conditions of the monitoring environment. The goal of this project was the development of an algorithm and user interface with the intent to enable BOEM personnel to input proposed array specifications and determine the theoretical localization capability for low-, mid-, and high-frequency cetaceans within 5 km of the array.

The parameters set by the project required the use of curved-wavefront localization (CWL), which is equivalent to hyperbolic localization in the time domain. Roughly speaking, a CWL becomes possible whenever a source is close enough to the array such that the apparent azimuth of the source will appear to vary along the array, when measured by pairs of adjacent hydrophones along the array. If expressed in terms of hyperbolic localization, CWL means that hyperbolas produced by pairs of hydrophones will eventually intersect and will not become asymptotically parallel at large ranges. The term "curved-wavefront localization" arises because, in order for an array to localize in range, the wavefront of a signal passing over an array cannot be a plane wave structure but must display curvature.

The fundamental approach of the algorithm development was to run multiple iterations of a marine mammal localization problem, randomly varying relevant parameters to estimate the bias and variance of the resulting range estimates. Each iteration generated a random realization of a marine mammal signal at each receiving hydrophone by randomly generating different source parameters, hydrophone positions, and the background noise time series. The simulated time series were then cross-correlated between hydrophones, and the desired localization algorithm applied. The process was repeated at all grid locations, and then additional iterations were conducted to build a distribution of range estimates from which the bias and variance of the range estimate can be computed for every grid point.

Two localization algorithms were applied, based on array geometries: a three-element case for the time-of-arrival algorithm, where the hydrophones can have any spacing, and a four-element case for the "cross-fixing" algorithm, where the hydrophones are divided into two pairs to form two short sub-apertures. For both approaches, the mean (unperturbed) positions of the hydrophone elements were used in the localization calculation. Localization algorithms that require a larger number of hydrophones were not modeled because the majority of existing systems do not use more than four hydrophones for localization during real-time mitigation monitoring, and because the determining factor for the range resolution of a system is the total aperture (i.e., maximum separation between array hydrophones). A maximum 5-km radius monitoring grid with 1-m resolution was used to evaluate localizations at each grid point of interest within the algorithm.

The algorithm was tested using a grid search method against the dataset published by Abadi et al. (2015, 2017). This dataset is key to the algorithm testing because it provides a peer-review standard that statistically correlates acoustic detections with visual observations. The algorithm was developed to enhance localization capabilities where no direct path exists between the source and receiver.

The main insight from these simulations was that the uncertainty in range estimation is dominated by the uncertainty in array element position, likely due to the fact that the specified noise levels are too low, having been derived for measurements from a stationary platform well away from vessel noise. The introduction of vessel noise in towed PAM array systems is expected to increase localization uncertainty when signals are detected. In consultation with BOEM, example background noise profiles from actual PAM operations will be explored to determine when background noise levels become a determining factor for PAM array performance, as a means to test simulations for conditions that may be present during offshore wind farm development.

The draft and final algorithm consists of a spreadsheet; a platform-independent, stand-alone software package; and a user manual. The spreadsheet contains the formulas from the study, so that the user can quickly determine whether a given towed array configuration has any chance of meeting the localization requirements of an application. The stand-alone software package is written in MATLAB but will be processed with the MATLAB compiler to generate a stand-alone application package that can be distributed on a royalty-free basis. The stand-alone application does not require MATLAB to be executable. The advantage of this approach is that the MATLAB compiler can generate versions compatible with most hardware platforms, including Microsoft Windows and Apple operating systems. It can also generate web-based versions and stand-alone versions on a desktop or laptop computer, so that BOEM could put the tool online for public use.

# Contents

# List of Figures

# List of Tables

# List of Abbreviations and Acronyms

| | |
|---|---|
| μPa | micropascal |
| 1-D | one-dimensional |
| 2-D | two-dimensional |
| 3-D | three-dimensional |
| AMP | Alternative Monitoring Plan |
| ANSI | American National Standards Institute |
| ASA | Acoustical Society of America |
| BOEM | Bureau of Ocean Energy Management |
| CWL | curved-wavefront localization |
| dB | decibel |
| ESA | Endangered Species Act |
| FFT | fast Fourier transform |
| FM | frequency-modulated |
| MMPA | Marine Mammal Protection Act |
| PAM | passive acoustic monitoring |
| PSD | power spectral density |
| re | referenced to |
| SL | source level |
| SNR | signal-to-noise ratio |
| $SPL_{rms}$ | root-mean-square sound pressure level |
| TDoA | Time Delay of Arrival |
| TL | transmission loss |
| TMA | time-motion analysis |
| TOA | time-of-arrival |

# 1 Introduction

Passive acoustic monitoring (PAM) is widely used to monitor for the presence of marine mammals around vessels and other platforms during offshore survey and construction activities that could negatively impact marine mammals. Specifically, PAM is used during these activities for mitigation monitoring in which pre-defined mitigation zones are monitored to reduce the risk of potential impacts. The priority of mitigation monitoring is to enable compliance personnel with the ability to detect and spatially localize marine mammals such that a mitigation decision can be made within minutes of the detection. The complexity of acoustic detection and localization is hindered by practical operational conditions that are common for mitigation monitoring. The main challenge of a mitigation PAM system is the fact that it is usually towed from a vessel that may or may not be fit-for-purpose and is often towing other equipment, operating sound sources, and working in patterns that are permit- and/or project-driven rather than designed to optimize PAM performance. Mitigation actions initiated by marine mammal calls detected with PAM can result in the project incurring significant costs associated with down time (i.e., responding to a mitigation action that typically includes reduction or even temporary stoppage of activities). Therefore, accurate localization of calls for mitigation decisions are important for both regulatory and operational success.

Mitigation under Bureau of Ocean Energy Management (BOEM) wind leases require that Alternative Monitoring Plans (AMPs) are developed for conducting high-resolution geophysical surveys during impaired visual conditions. AMPs typically employ enhanced visual tools and PAM to monitor for marine mammals during low visibility conditions. BOEM must ensure that the equipment and methodologies being proposed in the AMPs meet the detection and reporting requirements for Endangered Species Act (ESA) and Marine Mammal Protection Act (MMPA) consultation with cooperating agencies. BOEM also has the responsibility, as the Lessor, to provide assurance to the public that mitigation measures are being adequately employed and effective use of PAM equipment and data constitute an important part of the assurance. Acoustic detections and localizations have been the subject of qualitative assessments since PAM equipment has been deployed regularly for mitigation purposes over the last 10 to 15 years, but uncertainties in localization methods make it difficult for quantitative assessments to be conducted. When evaluating the efficacy of a PAM system, BOEM currently relies heavily on input from the PAM providers and operators regarding the performance of the system. However, monitoring reports often state the ability to localize a marine mammal call. Localization comprises two components of call detection: the ability to range (i.e., determine the distance of a marine mammal call from the PAM hydrophones) and the ability estimate a bearing to the call. The consistency and reliability of these reported ranges and bearings may be suspect due to variability in the equipment, conditions, and operator skill level.

The ability to localize a marine mammal call using PAM systems commonly deployed for surveys, such as those conducted to support offshore wind development, requires several conditions and assumptions. In order to localize, the call must first be detected. A detection's range will be dictated by the received amplitude of the signal (which in turn depends on the species, distance, and relative orientation to the receiver) as well as the noise conditions of the monitoring environment. Detection ranges from towed systems can be as small as 200 to 300 m for harbor porpoises (Cucknell et al., 2016) and as large as tens of kilometers for baleen whales and sperm whales (Hildebrand, 2009). Therefore, optimizing the ability to detect calls by using appropriate equipment and deployment methods will remain a priority in any assessment of localization capabilities.

## 1.1 Scope/Goals of Project

The goal of this project was to development an algorithm that allows BOEM to assess the localization efficacy of towed PAM arrays proposed in mitigation and monitoring plans for offshore wind farm development. The intent of the resulting algorithm and user interface was to enable BOEM personnel to input proposed array specifications to determine the theoretical localization capability for low-, mid-, and high-frequency cetaceans within 5 km of the array.

Because a variety of factors can affect localization efficacy and PAM performance, the approach to developing, testing, and delivering the algorithm required clarification of the assumptions, analysis of the relevant parameters, and development of a framework to incorporate the biological and physical parameters involved with evaluating efficacy of localization using PAM systems.

## 2 Approach and Methods

This section lists the requirements and assumptions specified for the analysis, provides an analysis of the key factors that determine range localization uncertainty, and details the algorithm and structure of the numerical evaluation code, which uses multiple simulations of various realizations of signals, noise, and array position to estimate positional uncertainty.

## 2.1 Requirements and Assumptions

BOEM had specific requirements for any numerical model of towed PAM array performance. This section summarizes these requirements, describes why some of the assumptions behind these requirements have been modified in the final effort, and discusses some important consequences of these assumptions when modeling localization methods. The original requirements provided by BOEM are as follows:

A. The array is assumed to be a single linear, flat array with a maximum of 20 hydrophones, each of which completely covers the entire frequency spectrum of any signals of interest.
B. Left-right bearing ambiguity is not a modeling concern.
C. Hydrophone spacing may not be uniform.
D. Acoustic environment is assumed to have an isovelocity sound speed of 1,500 m s$^{-1}$, with no multipath present to interfere with (or to be exploited by) localization methods.
E. Any propagation loss modeling should use a power law transmission loss, which will be 15log(R) for water depths less than 200 m, where R represents the range from the source. For deeper water depths, the propagation law will be 20log(R) for the first 1,000 m and then 10log(R) afterwards. Both scenarios should include absorption, the precise nature of which is not defined in the requirements.
F. The area to be monitored horizontally is up to a 5-km radius circle, with the origin at the midpoint (geometric center) of the linear array. A grid of at least 1-m resolution should be possible for localization evaluation.
G. The localization method should use time-of-arrival (TOA) processing, while accounting for potential errors in relative TOA estimates ranging from 1 to 100 ms.

H. Three categories of marine mammal species should be defined, each with a characteristic frequency bandwidth and source level (SL) for the calls (loudness: low-frequency [10 to 1,000 Hz; 140 to 190 decibels (dB) referenced to (re) 1 micropascal (µPa) @ 1 m], mid-frequency [1,000 to 20,000 Hz; 130 to 220 dB re 1 µPa m], and high-frequency [20,000 to 120,000 Hz; 130 to 180 dB re 1 µPa m]). The algorithm should also incorporate source directionality effects and repetition rate.

I. Ambient spectrum noise levels for various frequency bands are 75, 50, and 45 dB re 1 µPa for the low-, mid-, and high-frequency categories listed above. The units for these values are assumed to be root-mean-square sound pressure level ($SPL_{rms}$), integrated over the appropriate bandwidth of the marine mammal signal.

J. Signal detection thresholds over ambient noise should be between 0 and 20 dB.

K. Time Delay of Arrival (TDoA) techniques for a single received signal (which are assumed to be received on each hydrophone) should be used as the localization process for algorithm development.

During the algorithm development, some of the assumptions within these requirements were altered and clarified, in consultation with BOEM during the Task Order award meeting. A summary of the modifications are as follows.

Requirement A: The maximum number of hydrophones was limited to four, because existing practical PAM localization algorithms for towed arrays do not use more than this number, and **Section 2.2** demonstrates that the ranging capability of a PAM system is determined by the aperture (i.e., maximum distance between the end hydrophones) rather than the number of hydrophones. Algorithms for processing more than four hydrophones (Li et al., 2016) are also an order of magnitude slower than the analytic solutions employed here. It was also assumed that simulations did not need to consider multiple array systems deployed by a single platform or deployed across multiple spatially separated platforms.

Requirement E: Instead of the shallow/deep water power law transmission loss initially requested, a propagation law that was directly tied to the local water depth, $D$, was implemented. When the source range (i.e., R) was less than the water depth, the propagation loss was modeled as $20\log(D)$, but at greater ranges the loss was modeled as $20\log(D)+15\log(R/D)$. This formula is more physically accurate and ensures a smooth transition between the shallow and deep water cases. Absorption was also modeled as in-water attenuation caused by "Thorpe attenuation," as this is the absorption that is most important for mid- and high-frequency cetacean propagation loss.

Requirement G: Given that "localization" can refer to one-dimensional (1-D) estimates (azimuth of a signal), two-dimensional (2-D) estimates (range and azimuth), and three-dimensional (3-D) estimates (range, azimuth, and depth), localization was to be defined here as a 2-D fix (i.e., azimuth and slant range with respect to the center of the array), with no need to divide the slant range into a horizontal range and source depth, which generally requires either planar arrays or exploitation of acoustic multipath. It was also assumed that TOA (i.e., signal phase) information collected across the array aperture should be primarily used for localization, and it should not be attempted to exploit the relative amplitudes of the same signal detected on multiple array hydrophones. Any attempt to exploit relative amplitude requires a detailed and accurate propagation model that is beyond the scope of the BOEM request.

Requirement H: Instead of incorporating the three generic marine mammal categories, more specific "clusters" of marine mammal acoustic types were defined to be consistent with assumptions used by an upcoming Acoustical Society of America (ASA)/American National Standards Institute (ANSI) standard on towed PAM array operations, as well as with recent software developments to the open-source software PAMGuard. Variations in source directionality were modeled by increasing the spread of possible SLs generated within a species cluster.

Another important change made to this requirement was the decision not to model marine mammal vocalization repetition rates in the simulation. This was decided for several reasons:

- The BOEM requirements did not specify a time interval over which a sequence of sounds should be measured. Without these details the localization uncertainty assigned to a sequence of sounds could not be evaluated, because the number of sounds to be simulated could not be determined;
- Information on natural repetition rates of various marine mammal sounds is sparse, and what exists indicates that sound repetition rates depend strongly on the animal's behavioral state, time of day, and a host of other factors that could not be easily simulated. Instead, development of the algorithm focused on the localization uncertainty generated by a vocalization, under the assumption that such a vocalization was uttered; and
- The probability of detection and localization for a sequence of sounds could be derived from the Monte-Carlo approach used by the algorithm.

Requirement I: The noise levels specified seemed to arise from the classic wind-driven noise levels predicted by the "Wenz curves" (Wenz, 1962). Thus, an option was included to let the ocean sea state determine the noise levels as a function of frequency, instead of specifying noise levels directly.

Requirement K: This requirement placed important restrictions on the types of localization to be modeled. Specifically, Requirement K precluded modeling with the "time-motion analysis" (TMA) technique, which is a traditional and common method for localizing sources using towed PAM arrays. The TMA technique works by collecting measurements of a sequence of azimuths collected from multiple signals generated over a relatively short interval, where the towed PAM array has moved to different locations. TMA assumes the measured signal sequence originates from the same animal or compact group of animals. Triangulation of these bearings then provides a localization estimate. TMA is a very simple implementation of a more general concept called "synthetic aperture sonar," and sperm whales have been localized at ranges out to tens of kilometers using this technique. Despite its advantages, which include minimal hardware requirements and relatively simple implementation, the TMA method does require multiple, good quality signals and must assume that the source (animal or group) is stationary or slow-moving in a predictable direction, which is often not the case, especially for small odontocete species. Because Requirement K restricted techniques to those that work for a single signal (which is assumed to be received on each hydrophone), this implied that TMA methods should not be included in a performance algorithm, and therefore localization methods that involve detecting sound sequences were not considered further in this project, despite their common use in PAM systems.

As a result, the following analysis and simulations were limited to two methods that are currently used by existing practical towed PAM systems: relative TOA modeling and "cross-fixing." Both methods are discussed in more detail below.

## 2.2  Analytic Formulas for Maximum Localization Distance

Due to the aforementioned restrictions in equipment configuration and environment, the only technique available for localizing marine mammal sounds in both azimuth and range arose from curved-wavefront localization (CWL), which is equivalent to hyperbolic localization in the time domain. Roughly speaking, a CWL becomes possible whenever a source is close enough to the array such that the apparent azimuth of the source will appear to vary along the array when measured by pairs of adjacent hydrophones along the array. If expressed in terms of hyperbolic localization, CWL means that hyperbolas produced by pairs of hydrophones will eventually intersect and will not become asymptotically parallel at large ranges. The term "curved-wavefront localization" arises because, in order for an array to localize in range, the wavefront of a signal passing over an array cannot be a "plane wave" structure but must display curvature. Mathematically, the maximum range, $R_{max}$, that an array with span (i.e., aperture), $L$, can

intercept a curved wavefront (known in physics as the far-field or Fraunhofer condition) is shown in **Eq. (1)**.

$$R_{max} << D^2/l = L^2 f/c \qquad \text{Eq. (1)}$$

$$R_{max} \sim 0.1\, L^2 f/c/f$$

where $c$ is the speed of sound in water, $f$ is a typical acoustic frequency in Hz, and $l$ is the acoustic wavelength of frequency $f$ in a medium with sound speed $c$.

This equation describes an ideal situation where relative arrival times between hydrophones can be measured perfectly and exact hydrophone locations are also known. However, the equation illustrates the key point that the frequency of a signal and the size of the array are the fundamental factors that determine the ranging distance of a PAM array. As one moves from high-frequency odontocetes to low-frequency baleen whales, the length of the array needs to increase in order to maintain the same ranging capability. Thus, ranging low-frequency signals requires much larger array lengths than their higher frequency counterparts. The only publicly available datasets that are known to have towed arrays of sufficient length to demonstrate localization of baleen whales are seismic streamer data collected by the National Science Foundation, which have been analyzed in peer-reviewed literature (Abadi et al., 2015, 2017). The unique dataset analyzed by Abadi et al. (2015) serves as a key "known dataset" for testing and confirming the algorithm physics under contract requirements.

Besides array aperture ($L$) and signal wavelength, other sources of uncertainty exist that degrade this upper limit on performance, including uncertainties in signal timing measurements and hydrophone position.

Mathematically, most marine mammal signals can be defined as pulses, frequency-modulated (FM) sweeps, or short-duration tones, with most sounds represented as FM sweeps. An analytical concept called the Cramer-Rao Lower Bound provides a classic method for estimating the lowest possible uncertainty of an acoustic measurement (or any signal processing measurement) for various levels of background noise. The timing uncertainty in estimating the TOA of an FM signal at a hydrophone (when referenced to an adjacent hydrophone) is given by the Cramer-Rao Lower Bound as **Eq. (2)** (Skolnik, 1962):

$$\delta t = \frac{1}{\pi f_B} \sqrt{\frac{3}{8*SNR}} \qquad \text{Eq. (2)}$$

Here, SNR is the signal-to-noise ratio of the signal, and $f_B$ is the effective frequency bandwidth of the call (i.e., the difference between the minimum and maximum frequencies of the call where a significant portion of the energy falls). The SNRdB, in turn, is provided by **Eq. (3)** (expressed in dB units):

$$\text{SNRdB} = \text{SL} - A\log_{10}(\text{R}) - N\text{dB} + AG \qquad \text{Eq. (3)}$$

where SL is the source level of the signal in units of dB re 1 μPa m, $A$ is a propagation factor for modeling propagation loss, $N$dB is the noise level computed across the signal bandwidth, and $AG$ is the potential array gain that arises when multiple hydrophones are used to enhance a signal. When computed, the value of SNRdB is then converted into a linear SNR estimate by calculating $10^{(SNRdB/10)}$, which is then applied to **Eq. (2)**.

Mathematically, the maximum range $R_{max}$ that an array with length (aperture) $L$ can localize using CWL is shown in **Eq. (4)**.

$$R_{max} = L^2 \big/ 2c\delta t \qquad \text{Eq. (4)}$$

Thus, for an FM sweep signal (and broadband pulses), the result is a relatively simple formula for predicting the useable localization range of a towed array:

$$R_{max} = \frac{\pi f_B L^2}{c} \sqrt{\frac{2\text{SNR}}{3}}$$

Eq. (5)

Based on this equation, the localization capability of an array increases as its length increases and as the signal bandwidth and SNR increase. Similar formulas exist for tonal sounds.

**Eq. (5)** is most accurate for high frequencies where the bandwidth is a fraction of the center frequency; as the frequency decreases toward baleen whale frequencies, and where the measurement error becomes small relative to an acoustic wavelength, the result converges into **Eq. (1)**. A 100-Hz signal would thus need an array length of nearly 1 km to localize out to the 5-km range, using the assumptions listed in **Section 2.1**. Although it is unlikely that any towed PAM array used for mitigation for offshore wind farm development will achieve that length, a dataset capable of conducting CWL with a single towed array was included to verify the performance of the algorithm over lower-frequency (as well as high-frequency) signals.

These equations provide a quick and simple way to check whether a given array configuration can achieve the ranging capability required.

## 2.3  Algorithm Description

This section describes the specific numerical algorithm for estimating the range uncertainty of marine mammal calls. The fundamental approach of the algorithm was to run multiple iterations of a marine mammal localization problem at every localization grid point of interest while randomly altering various relevant parameters to estimate the bias and variance of the resulting range estimates. Each iteration generated a random realization of a marine mammal signal at each receiving hydrophone by randomly generating different source parameters, hydrophone positions, and background noise time series. The simulated time series were then cross-correlated between hydrophones, and the desired localization algorithm was applied, assuming perfect knowledge of hydrophone position (even though the simulated hydrophone positions might have been slightly offset from the desired positions). The process was repeated at all grid locations, and then additional iterations were conducted to build a distribution of range estimates from which the bias and variance of the range estimate could be computed for every grid point. This process automatically incorporated all sources of uncertainty into the prediction and permitted the impact of particular sources of uncertainty (time delay, hydrophone position) to be isolated and evaluated.

For the following sections, the numerical algorithm is subdivided into several components: array and environmental geometry, species cluster signal, propagation, noise, localization, and metrics. Specific input variables that the user can control are identified using ***italic bold*** type, with the appropriate units and default value (if it exists) provided in parentheses. Intermediate variables derived inside the algorithm from these inputs are designated by plain *italic* type.

### 2.3.1  Array and Environmental Geometry

The model assumes an ocean with constant depth **D** (m) and isovelocity sound speed **c** (1,500 m/s). A rectangular grid with at least 1-m spacing encompasses a circular region of **R**_*max* (5 km) radius. The array is arranged along the x-axis, with its geometric center defined to be the coordinate origin. Two array geometries are permitted: a three-element case (i.e., TOA modeling), where the hydrophones can have any spacing, and a four-element case (i.e., cross-fixing), where the hydrophones are divided into two pairs

to form two short sub-apertures $L_1$ and $L_2$, separated by a baseline distance $B$. In both cases the total array length $D$ (in meters) is derived from the individual array element positions.

Each of $N$ hydrophones, numbered with index $i$, is assigned a mean position $x_{i,mean}$ (m) along the x-axis, with a value of zero along the y-axis. Each hydrophone is also assigned a positional uncertainty $\sigma_x$ (m). For the TOA geometry, each hydrophone $i$ is assigned an individual random angle $\theta_i$ selected from a uniform circular distribution (-180°, 180°) and a displacement $\Delta r_i$ selected from a normal distribution with zero mean and standard deviation $\sigma_x$. The true position of hydrophone $i$ therefore becomes:

$$x_i = x_{i,mean} + \Delta r_i \cos\theta_i, \; y_i = \Delta r_i \sin\theta_i \qquad \text{Eq. (6)}$$

For the cross-fixing case, only one of each pair of hydrophones is adjusted using **Eq. (6)**. The position of the second hydrophone in the pair $(i+1)$ is then defined by:

$$x_{i+1} = x_i + L\cos\theta_{i+1}, \; y_i = L\sin\theta_{i+1} \qquad \text{Eq. (7)}$$

where $\theta_{i+1}$ is selected from a uniform distribution with domain (-$\theta_{max\_yaw}$, +$\theta_{max\_yaw}$). **Eq. (7)** ensures that the aperture across the sub-aperture remains fixed, but that the yaw angle (i.e., the angle formed between the line connecting the subarray hydrophones and x-axis) can vary between the subarrays. The motivation for this logic is that hydrophones in a subarray are usually within a couple of meters of each other, and so their relative position is nearly fixed. However, the relative position of two subarrays across baseline distance $B$ can vary due to the large value of the baseline, and a towed PAM array often wanders in the yaw angle, particularly at low tow speeds.

The possibility was considered of permitting the hydrophone uncertainty parameters to vary as a function of array tow speed, with a PAM array towed at a faster speed displaying smaller positional uncertainties, but it was ultimately decided that computing this relationship from first principles was too involved and would require knowledge of array cable properties (e.g., diameter, density, coefficient of friction) that most PAM users would not know. Thus, the final input parameters characterizing positional uncertainty are set directly.

As no multipath effects are incorporated into the simulation, the depth of the towed array becomes irrelevant and is not an input parameter.

### 2.3.2 Species Cluster Signal

The initial BOEM requirements specified SLs and bandwidths for three general categories of marine mammal species (Requirement H). Instead, the algorithm provided the option for subdividing cetacean calls into nine "clusters," with more sharply defined bandwidths, SLs, and SL variabilities. **Table 1** displays the details behind these clusters, which is adapted from a proposed ASA/ANSI standard for towed PAM array monitoring, as well as a simulation model for the open-source bioacoustic detection software package PAMGuard. The reason for providing this additional level of specificity is that the uncertainty in a TDoA measurement is highly dependent on the exact bandwidth, duration, and SL of the modeled signal, as well as the uncertainties associated with these parameters, and thus subdividing the vast variety of marine mammal signals into more detailed clusters was appropriate. SLs were expressed as $SPL_{rms}$, because that is the most frequent unit provided in the literature (Erbe et al., 2017).

Whenever the numerical software within the algorithm requested a realization of a particular cluster sound during a particular iteration, it selected duration and frequency parameters from a uniform distribution, whose limits are defined in **Table 1** for each species cluster. The SL was drawn from a normal distribution with the standard deviation as specified in **Table 1**. After selection, these parameters remained fixed while evaluating all location grid points during that iteration.

The effective bandwidth of the signal is of crucial importance when determining the TDoA uncertainty. For FM sweep signals, the minimum and maximum frequencies are determined directly from the parameters (**Table 1**). For pulse sounds (e.g., sperm whales), whose energy tapers off gradually with frequency, the bandwidth is determined by the spectral points that fall 20 dB below the maximum source spectrum.

After the specific parameter values were selected, the algorithm program generated a time series of duration, $T$, using the specified sampling rate of the recording system, $F_s$, to generate $N_t$ discrete samples with amplitude units of µPa. In most cases, the algorithm program assigned a default value of $F_s$ based on the species cluster selected.

**Table 1.    Summary of species cluster acoustic categories used in the study**

| Name (Abbreviation; Color) | Core Detection Bandwidth (Hz) | Apparent Source Level Distribution dB re 1 µPa m (expressed as SPL$_{rms}$) | Time Series Test Implementation |
|---|---|---|---|
| Low-frequency baleen whales (LFBW; red) | 20–100 | 189 ± 10 | Random linear FM sweep between 15–100 Hz. Sweep is restricted to 1 octave (e.g., can sweep from 15–30 Hz, or from 50–100 Hz, but not from 15–100 Hz in one go). Duration 2–10 ± 0.5 s. |
| High-frequency baleen whales (HFBW; orange) | 50–1,000 (humpback) 50–500 (bowhead) | 160 ± 10 (song) 137 (social) | Random linear FM sweep between 50 and 1,000 Hz. Restricted to 1.5 octaves. Duration 2 ± 0.5 s. |
| Right whales (RW; yellow) | 75–300 (upcall) 30–8,400 (gunshot) | 175 ± 2.5 | Shape is a quadratic FM sweep with three points drawn from frequency distributions of 90 ± 15, 110 ± 20 and 170 ± 30. Duration 0.75 ± 0.25 s. |
| Sperm whale (SW; green) | 2,000–24,000 | 186 ± 3 (usual), 171 ± 5 (creaks) | 5–6 cycles of sound generated between 5–10 kHz. Duration ~1 ms. Hann windowed. |
| Beaked whales (BW; blue) | 20,000–96,000 (includes frequency band between 80,000–96,000 for detection enhancement) | 180 ± 9 | Linear up-sweep between two distributions from starting frequency 20 ± 5 kHz, to ending frequency 45 ± 5 kHz. Duration 0.3 ± 0.03 ms. |
| Blackfish (BF; indigo) | 4,000–8,000 | 122 ± 4 | Random sweep between 4–8 kHz, restricted to 0.6 octaves. Duration 0.4 ± 0.01 s; 7 square wave harmonics. |
| Dolphin tonals (DT; violet) | 2,000–24,000 | 148 ± 13 | Linear chirps between 2–24 kHz. Restricted to 1.5 octaves. No harmonics. Duration 0.5 ± 0.2 s. |
| Dolphin clicks (DC; violet cross-hatched) | 10,000–100,000 | 162 ± 10 | Single cycle pulse at 60 kHz (gives a click with a bandwidth of about 3–120 kHz). |
| High-frequency cetaceans (HF; black) | 110,000–180,000 120,000–150,000 Hz | 165 ± 13 | Harbor porpoise chosen as representative species. Frequency at 130 ± 5 kHz, windowed with a raised sine wave. Duration 77 ± 7 µs. |

dB = decibel; FM = frequency-modulated; µPa = micropascal; re = referenced to; SPL$_{rms}$ = root-mean-square sound pressure level.

### 2.3.3  Propagation

As requested by Requirement E, acoustic propagation loss, or transmission loss (TL), was modeled by a power law; however, two modified formulas, **Eq. (8)**, were used:

$$TL = 20\log10(R), R < \boldsymbol{D}$$

$$TL = 20\log10(\boldsymbol{D}) + 15\log10(R/\boldsymbol{D}), R > \boldsymbol{D} \qquad \text{Eq. (8)}$$

where R is the modeled horizontal range to the source, and $\boldsymbol{D}$ is the water depth specified in the previous section. These formulas automatically compensate for the effect of water depth and permit a smooth transition from "spherical" (open-water) spreading to "practical" (bottom-interacting) spreading when moving from short to longer ranges.

An additional propagation effect incorporated into the simulation was in-water absorption, a factor that becomes important for mid- to high-frequency (*f*) sounds. The formula is adapted from Ainslie and McColm (1998) and is as follows:

$$f1 = 0.78e^{T/26}\sqrt{S/35}$$

$$f2 = 42e^{T/17}$$

$$A_{boric} = 0.106e^{(pH-8)/0.56}\frac{f_1 f^2}{f_1^2 + f^2}$$

$$A_{magnesium} = 0.52(1 + T/43)(S/35)e^{-D/6}\frac{f_2 f^2}{f_2^2 + f^2}$$

$$Attenuation\ (\tfrac{dB}{km}) = A_{boric} + A_{magnesium} + 0.00049f^2 e^{-\frac{T}{27} - \frac{D}{17}} \qquad \text{Eq. (9)}$$

where the temperature *T* is modeled as 10°C, the water salinity *S* is 35 practical salinity units, the water pH is *8*, and the water depth is taken to be the ocean depth $\boldsymbol{D}$.

To incorporate propagation effects, the source signal time series from the previous section was scaled according to the TL using the range computed from each grid point to each hydrophone. Water absorption was added by computing the Fourier transform of the received signal, applying the frequency-dependent water attenuation factor from **Eq. (9)**, and then applying the inverse Fourier transform.

### 2.3.4  Noise

Input noise levels are in terms of power spectral density (PSD), the most fundamental metric for characterizing a noise spectrum, because all other noise metrics (e.g., octave level, one-third octave level) can be derived from PSD. The dominant noise factor for towed PAM arrays is typically the towing platform itself; however, every tow platform has a unique noise spectrum, which is typically unknown until PAM operations begin.

The model permits two input options for the background noise level:
1) A customized noise spectrum can be entered as two vectors: $\boldsymbol{f_{noise}}$ and $\boldsymbol{PSD_{noise}}$, which represent the noise frequency and noise PSD levels, respectively; and
2) If the towing platform noise spectrum is unknown, a background noise model is derived using the Wenz curves that characterize historical noise levels as a function of frequency, *Beaufort force*, and qualitative "*shipping level*." **Figure 1** illustrates the curves and their dependence on these factors, where the sea state is roughly one less than the *Beaufort force*. The noise levels provided in Requirement I are consistent with the Wenz curves when integrated over bandwidths representative for each category.
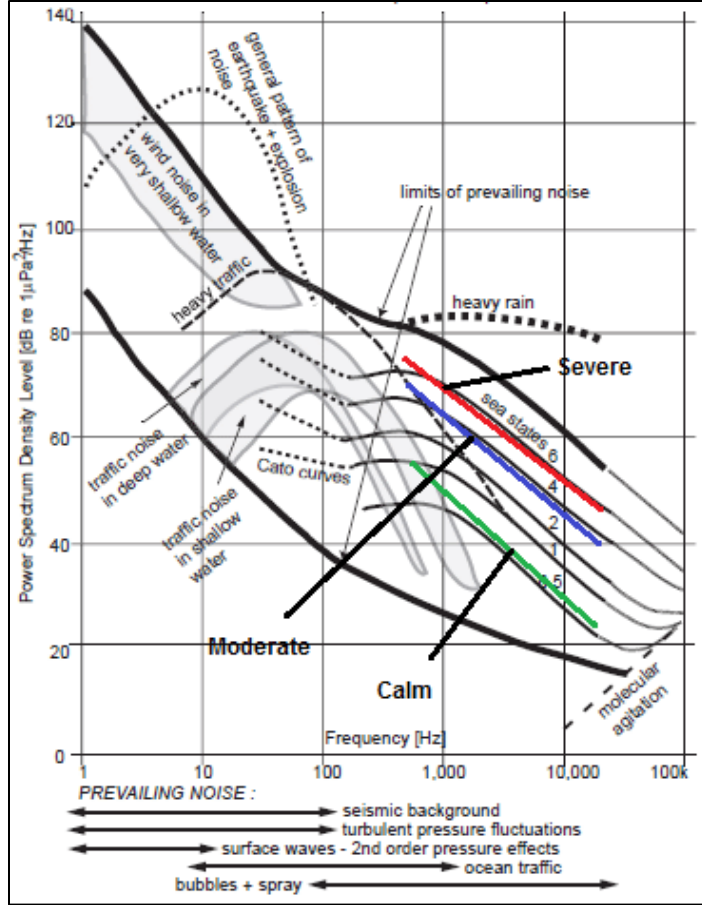
**Figure 1.** **The noise Wenz curves included in the simulation, characterized by sea state (Beaufort force minus 1) and shipping level**
Based on work by Wenz (1962).

The first input option, if available, is preferred because the Wenz noise levels are derived for stationary hydrophones situated away from nearby vessels (although the influence of regional shipping activity can be modeled). Wenz noise levels are thus unrealistically low for typical PAM operations. However, the second input option is made available given the need for practicality and data availability for personnel in mitigation programs.

After the PSD was defined along a set of evenly spaced frequencies, a random noise time series was generated by assigning a random phase to each frequency component, taking the inverse fast Fourier transform (FFT) of the square root of the PSD (expressed in linear units), and providing the appropriate scaling factor so that Parseval's Theorem [**Eq. (10)**] holds:

$$\int_0^{F_s} PSD(f)\, df = \int_0^T x_{noise}^2(t)dt \sim \sum_i PSD_i \left(\frac{F_s}{N_t}\right) = \frac{1}{T}\sum_i x_{i,noise}^2 \Delta t \qquad \text{Eq. (10)}$$

where $F_s$ is the simulated sampling frequency of the recording system, and $N_t$ is the number of samples desired for the noise sample, both of which are determined by the source signal. The time interval between samples, $\Delta t$, is $1/F_s$, and the total duration of the time series is $T=N_t \Delta t$. Specifically [**Eq. (11)**]:

$$x_{noise}(t) = \sqrt{2F_s N_t}\,\text{FFT}^{-1}[PSD] \qquad \text{Eq. (11)}$$

where FFT$^{-1}$ represents the inverse FFT. The mean value of $x_{noise}(t)$ is then subtracted from the time series to ensure no direct current bias (i.e., "leakage" into estimates of the low-frequency spectrum when using an FFT) contaminates the simulation. The resulting noise time series was bandpass filtered to match the bandwidth of the source signal (as defined in **Section 2.3.2**) and then added to the scaled and adjusted received source time series generated as described in **Section 2.3.3**. The noise bandwidth was set to the signal bandwidth in the expectation that a real PAM system operator or automated detector would attempt to filter the signal before localizing to reduce as much extraneous noise as possible. The same realization of the noise time series was applied to all grid points tested during a given iteration (although the amplitude and structure of the source signal will vary).

### 2.3.5  Localization

After a given source signal and filtered noise sample were combined to generate a set of received signal time series, the results were cross correlated with each other to produce a direct estimate of the time delays between all pairwise hydrophone elements. The peak of the cross-covariance function was then interpreted as the relative time delay between the hydrophones. This approach automatically removed the need for a user to specify the signal's SNR or TDoA estimation uncertainty, because the simulated time series automatically incorporated these factors when the cross-correlation operation took place. The user also did not need to specify a detection threshold cutoff because if the detection threshold is not met, the resulting ensemble of localization estimates were either unphysical or display nearly random estimates.

One of two localization algorithms was then applied to these relative TOA estimates:
1. The TOA algorithm that uses the relative TDoA between three hydrophones to analytically estimate the range and bearing of the source using closed-form equations. The use of an analytic formula (Spencer, 2007) speeds up the simulation tremendously; or
2. The cross-fixing algorithm that uses the relative TDoA within a two-hydrophone sub-aperture to estimate an azimuthal bearing. Bearings $q_1$ and $q_2$ from two apertures separated by a baseline $B$ are then triangulated to estimate a position [**Eq. (12)**]:

$$R_i = B sin(\theta_1)/sin(\theta_1 - \theta_2) \qquad\qquad \text{Eq. (12)}$$

For both algorithms, the mean (unperturbed) positions of the hydrophone elements were used in the localization calculation to simulate the impact of uncertainties in array element position.

Localization algorithms that require a larger number of hydrophones were not modeled because the majority of existing systems do not use more than four hydrophones for localization during real-time mitigation monitoring, and because the determining factor for the range resolution of a system is the total aperture (i.e., maximum separation between array hydrophones), as can be seen from **Eqs. (1)** and **(5)**. In addition localization algorithms that use more than four hydrophones require time-consuming brute-force or gradient search optimization methods (Li et al., 2016).

### 2.3.6  Error Metrics

After a simulation is run $N_{iter}$ times, each localization grid point will have $N_{iter}$ range estimates ($R_{est}$), which vary due to the natural variation in marine mammal SLs, noise realizations, and array hydrophone positions. Two valuable metrics are derived from this distribution: the relative bias $R_{bias}$ and relative standard deviation $R_{std}$. If $R_{true}$ is the actual location of a modeled source measured relative to the unperturbed location of the reference hydrophone [**Eq. (13)**], then:

$$R_{bias} = |\langle R_{est}\rangle - R_{true}|/R_{true} \qquad\qquad \text{Eq. (13)}$$

where $<R_{est}>$ is the average of the range estimates, and:

$$R_{std} = \sqrt{|\langle(R_{est} - \langle R_{est}\rangle)^2\rangle|}/R_{true} \qquad \text{Eq. (14)}$$

**Eq. (14)** provides the variance. Any solutions that yielded an unphysical result (e.g., an imaginary position or negative range) were excluded from the calculations, unless all results are unphysical, and then the metrics were assigned a value of infinity.

The original request from BOEM suggested "positional error as a fraction of range for different range bins" as one appropriate metric captured by $R_{bias.}$ The bias measures the accuracy of the range estimate at that location. $R_{std}$ is also a valuable metric in that it shows how uncertain or variable the estimate can be. **Section 3.1** will demonstrate how an estimate can have low bias but high uncertainty because small perturbations in array geometry or other parameters get magnified into large changes in estimated position.

## 2.4  Algorithm Testing

The algorithm was tested against the dataset published by Abadi et al. (2015, 2017). This dataset is key to the algorithm testing because it provides a peer-review standard that statistically correlates acoustic detections with visual observations. Abadi et al. (2015, 2017) used a grid search method that utilized a seismic streamer array to estimate the range of low-frequency sound sources such as vocalizations from baleen whales. The seismic streamer used in this study is an 8-km horizontal array comprised of 636 hydrophone channels spaced 12.5 m apart. Seismic streamers, such as those used in this dataset, are designed to minimize the horizontal arrivals to focus on the acoustic energy bouncing back from the seafloor; thus, the algorithm was developed to enhance localization capabilities where no direct path exists between the source and receiver. This grid search method consisted of the following steps:

1.  The streamer was divided into smaller subarrays with or without overlaps;
2.  Travel time between a given trial location and the subarrays are calculated by dividing the distance by the horizontal propagation velocity, which is a projection of the average speed of sound onto the horizontal plane. To calculate the horizontal propagation velocity, beamforming was used to calculate the elevation angle (i.e., the angle between the arrival path and the vertical axis). The beamformer output limits the search area to the region inside the arriving paths;
3.  Observed travel time between the source location and the subarrays was estimated by cross correlation between the signal recoded by a selected hydrophone on the subarray and the signal received by a reference hydrophone;
4.  To minimize the error between the calculated travel time and the arrival time observed in data, the estimated source location was determined to be where the root-mean-square travel time residual of the relative arrival times for all subarrays was at the minimum; and
5.  The localization uncertainty was estimated from confidence levels in the spatial residual function assuming the vocalizations detected in a given time period were from the animals within a group swimming relatively close to each other so that the signals can be assumed to be generated from the same location.

## 2.5  Algorithm Products

The draft and final algorithm consists of a spreadsheet; a platform-independent, stand-alone software package; and a user manual. The spreadsheet contains the formulas from **Section 2.2** so the user can quickly determine whether a given towed PAM array configuration has any chance of meeting the localization requirements of an application. The stand-alone software package is written in MATLAB but will be processed with the MATLAB compiler to generate a stand-alone application that can be distributed on a royalty-free basis. The stand-alone application package does not require MATLAB to be

executable. The advantage of this approach is that the MATLAB compiler can generate versions compatible with most hardware platforms, including Microsoft Windows and Apple operating systems. It can also generate web-based versions and stand-alone versions on a desktop or laptop computer, so that BOEM could put the tool online for public use if needed.

# 3 Results

Two sets of results are provided: a series of simulations for a small, 200-m aperture towed PAM array, and an analysis of actual data from towed seismic survey streamers to illustrate the challenges of localizing low-frequency baleen whales.

## 3.1 Simulation Demonstrations

In the following demonstrations, the performance of a towed array with 200-m total aperture for three species clusters was simulated: sperm whale, right whale, and beaked whale. For the TOA geometry, a three-hydrophone case was used with an even 100-m separation along the horizontal (x) axis, while for the cross-fixing geometry, a four-element case was used arranged as two sub-apertures separated by 200 m along the horizontal axis, with each hydrophone pair within a subarray being 3 m apart. For all cases, the water depth ($D$) was set to 1 km and the maximum ranges ($R_{max}$) to 5 km, with a grid spacing of 100 m. Only positive values needed to be plotted along the x- and y-axis because the symmetry of the geometry ensures that the other four quadrants are simply mirror images of the quadrant plotted. The 5-km maximum range was selected to be consistent with Requirement F in **Section 2.1**. Ambient noise was modeled using the Wenz curve, assuming a Beaufort Sea (*Beaufort force* minus 1) state of 3 with low *shipping levels*. The SPL$_{rms}$ of the noise quoted below were derived by integrating the noise PSD over the representative bandwidth. Each individual iteration, however, generated slightly different signal bandwidths and thus experienced slightly different noise levels. As noted earlier, the noise levels reported here are likely unrealistically low for a towed platform, even for an autonomous underwater towed platform.
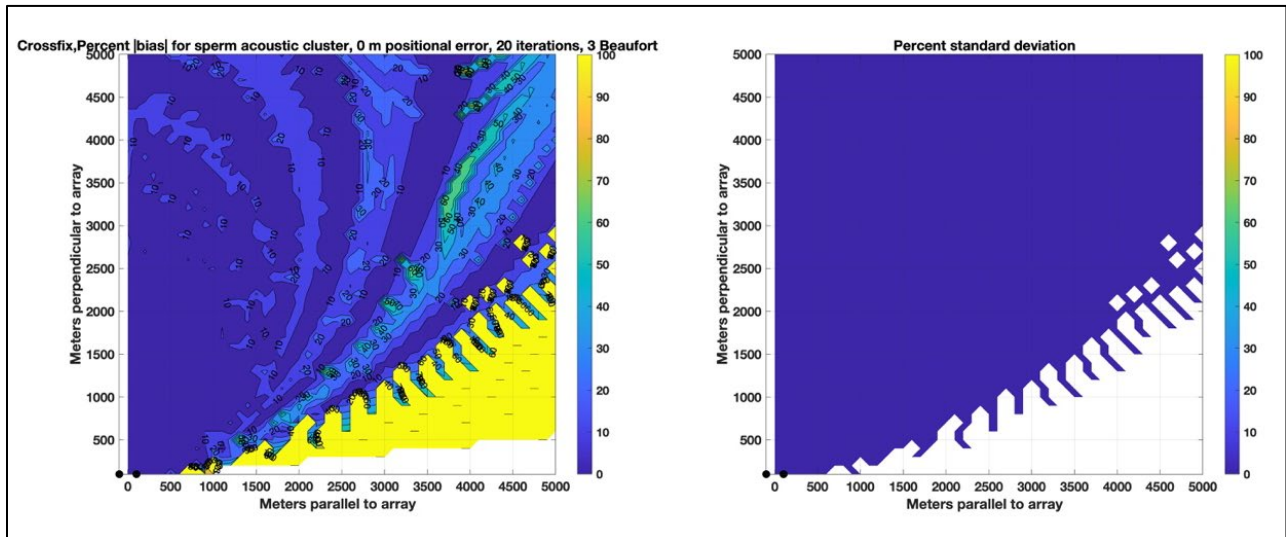
### 3.1.1 Sperm Whale

The sperm whale is one of the most common species detected offshore and for that reason has been assigned its own cluster in **Table 1**. **Figure 2** shows the results of performing 20 iterations of a sperm whale scenario for the three-element case, and **Figure 3** shows the corresponding four-element sub-aperture case, in a scenario where the array positions are assumed perfectly known, so any performance degradation arises from the physical limitations discussed in **Section 2.2**, along with the influence of the wind-driven noise levels. The system acoustic sampling rate ($F_s$) is assumed to be 48 kHz, and SPL$_{rms}$ of the noise is 82 dB re 1 µPa when integrated over the 6 to 12 kHz frequency band. For each figure, the left subplot shows a contour map of the relative bias (**Eq. 13**), while the right subplot displays the relative standard deviation of the 20 trials (**Eq. 14**), expressed as a percentage (**Eqs. 13** and **14** multiplied by 100). Under these circumstances, the theoretical performance of the system is excellent perpendicular ("broadside") to the system, but the bias degrades forward of the array (along the positive x-direction). White areas indicate locations that generate no valid solutions.

**Figure 3** shows that the cross-fixing algorithm has higher biases than the TOA algorithm (**Figure 2**) in the forward direction, but similar uncertainties.
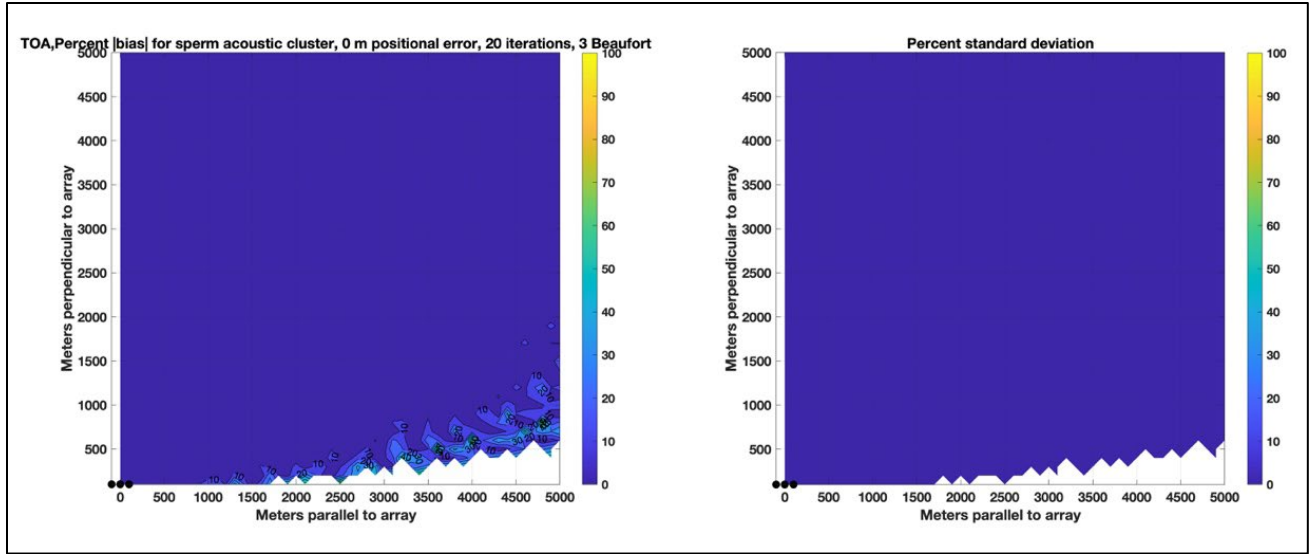
**Figure 2.** **Relative bias (left) and variance (right) expressed as a percentage, for 20 iterations of sperm whale scenario for the three-element time-of-arrival (TOA) localization geometry with no hydrophone localization uncertainty**
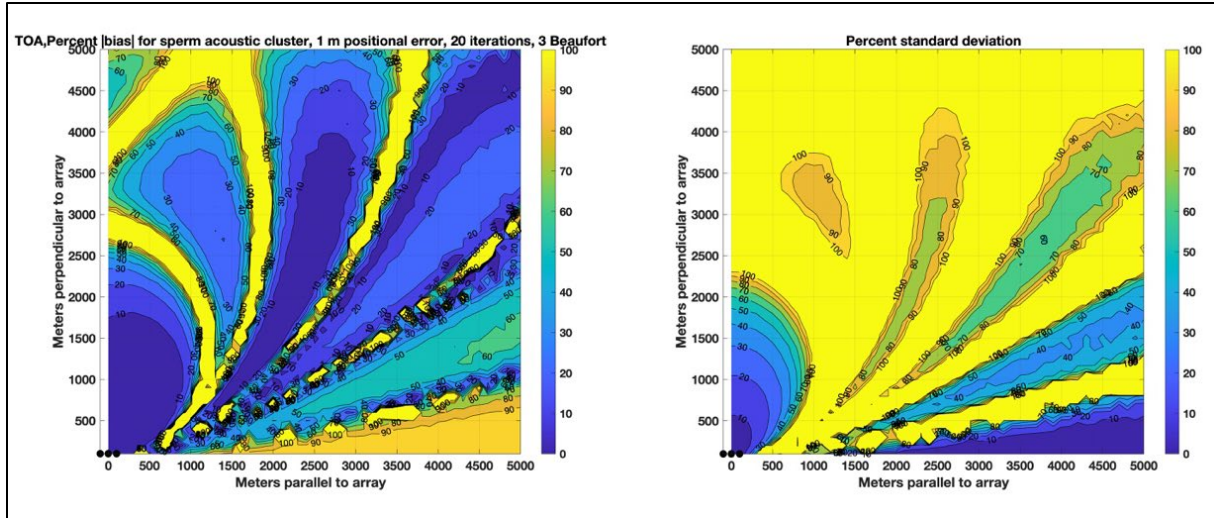
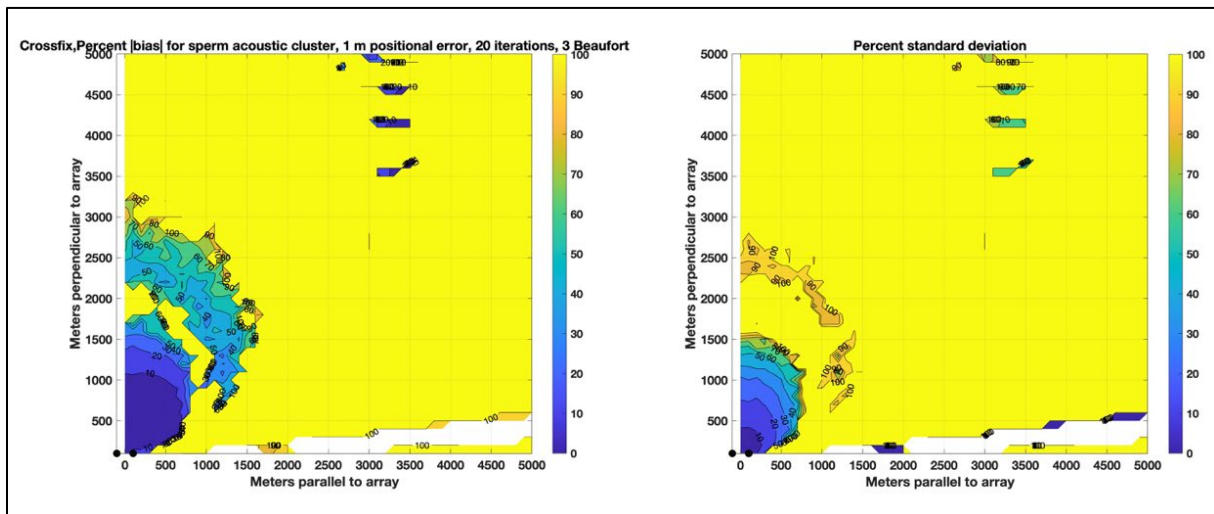Small black circles indicate hydrophone positions. White areas indicate locations with no valid solution.



**Figure 3.** **Relative bias (left) and variance (right) expressed as a percentage, for 20 iterations of a sperm whale scenario using the four-element cross-fixing localization algorithm, with no hydrophone localization uncertainty**

Small black circles indicate hydrophone positions. White areas indicate locations with no valid solution.

**Figures 4** and **5** show the impact of including a 1-m relative uncertainty in the towed PAM array positions, a value judged to be representative of most PAM situations particularly from slow-moving platforms and autonomous vehicles. **Figure 4**, which shows results of the three-hydrophone TOA algorithm, incorporates a 1-m uncertainty for all positions, while **Figure 5** , which shows results of the four-hydrophone cross-fixing algorithm, uses a 1-m uncertainty in relative subarray position and a $\pm 10°$ uncertainty in subarray heading, as discussed in **Section 2.3.1**.

14

**Figure 4.** Relative bias (left) and variance (right) expressed as a percentage for 20 iterations of a sperm whale scenario for the three-element time-of-arrival (TOA) localization geometry, incorporating 1-m uncertainty in hydrophone position

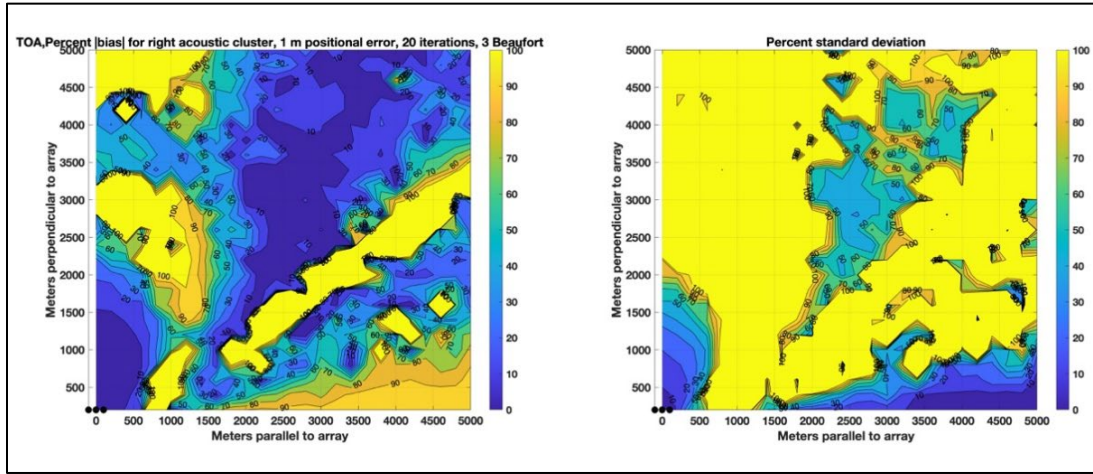Small black circles indicate hydrophone positions. White areas indicate locations with no valid solution.



**Figure 5.** Relative bias (left) and variance (right) expressed as a percentage for 20 iterations of a sperm whale scenario using the four-element cross-fixing localization algorithm, incorporating 1-m uncertainty in hydrophone position and 10° uncertainty in subarray heading

Small black circles indicate hydrophone positions. White areas indicate locations with no valid solution.

The degradation in array performance is apparent in **Figures 4** and **5**, with biases less than 50% existing only broadside of the array, and only out to 2.5 km for the TOA algorithm and 1.5 km for the cross-fixing algorithm. Note, however, that for the standard deviation to be less than 50% of the true range, the true range must be less than 1.8 km for the TOA algorithm or 1.25 km for the cross-fix algorithm. **Figure 4** also shows regions of relatively low bias at higher ranges and cross-ranges
(e.g., x = 2.5 km, y = 2.5 km), but these regions have high uncertainties and variability, indicating that the results are extremely sensitive to small errors in hydrophone position. Array position uncertainty was found to be the factor that has the largest impact on performance, so for the remaining species in this section, the array positions will be modeled with a 1-m uncertainty.
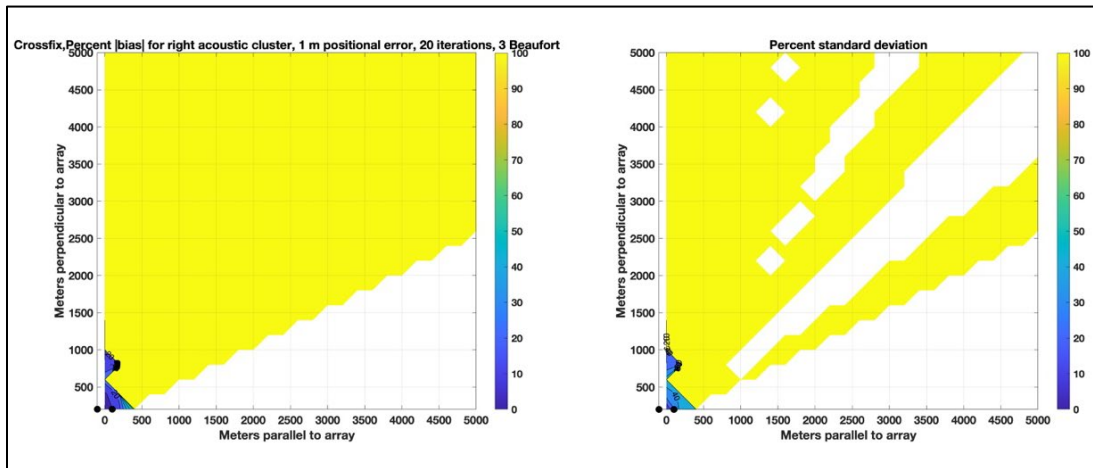
### 3.1.2  Right Whale

Localization of North Atlantic right whale calls are a high priority for PAM systems because the species is critically endangered and is afforded enhanced protection and mitigation measures when detected. Right whale FM signals occupy much lower bandwidths than sperm whale signals, so the simulations used a sampling rate ($F_s$) of 2.5 kHz in order to reduce computation time. The noise $SPL_{rms}$ was 80 dB re 1 µPa when integrated over the 100 to 170 Hz frequency band. **Figures 6** and **7**, which show results of the TOA and cross-fixing scenarios, indicate that a 200-m aperture towed PAM array might localize a right whale FM signal broadside of the system out to 1.5-km range with a 20% bias, but with a 40% standard deviation in range. The cross-fixing geometry, which relies on estimating bearings from two hydrophones 3 m apart, shows no ability to localize when the relative subarray heading uncertainty is 10° (**Figure 7**).



**Figure 6.**  Relative bias (left) and variance (right) expressed as a percentage for 20 iterations of a simulated right whale signal for the three-element time-of-arrival (TOA) localization geometry, incorporating 1-m uncertainty in hydrophone position

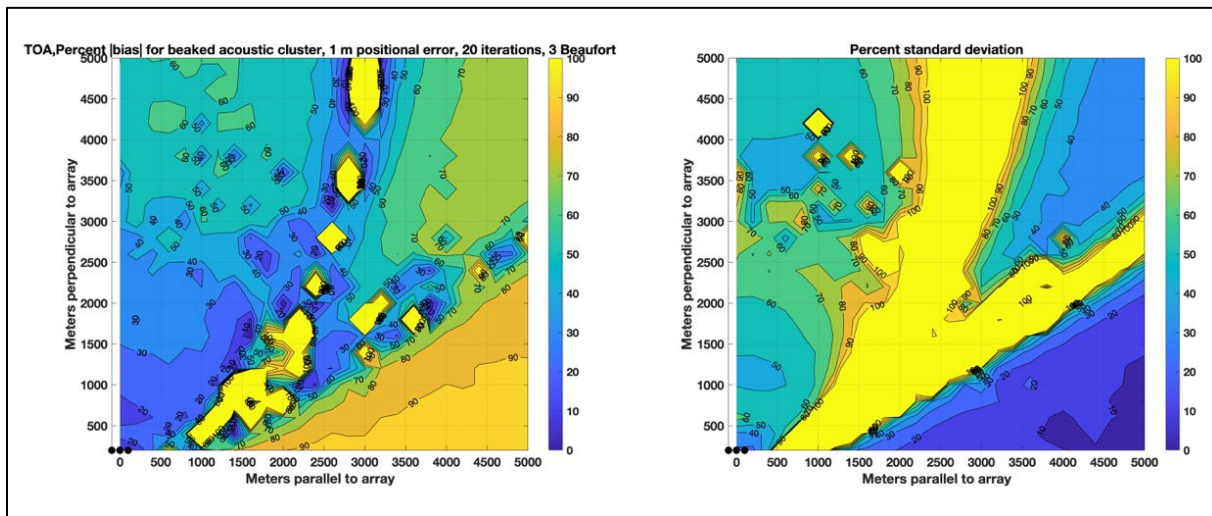Small black circles indicate hydrophone positions. White areas indicate locations with no valid solution.



**Figure 7.**  Relative bias (left) and variance (right) expressed as a percentage for 20 iterations of a simulated right whale signal using the cross-fixing localization algorithm, incorporating 1-m uncertainty in hydrophone position and 10° uncertainty in subarray heading
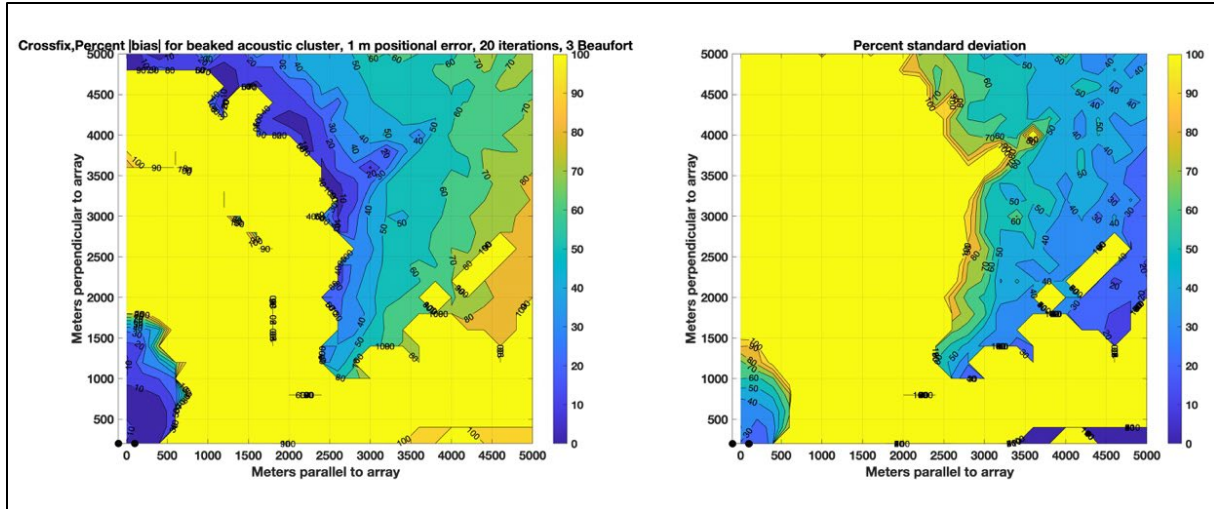
Small black circles indicate hydrophone positions. White areas indicate locations with no valid solution.

16

### 3.1.3  Beaked Whale

Another cluster of species of interest to PAM systems are beaked whales. Although unlikely to be encountered in shallow continental shelf waters, they have been detected on acoustic surveys off the U.S. eastern seaboard in deeper waters. For the simulation, the signal sampling rate ($F_s$) was set to 192 kHz, with noise SPL$_{rms}$ generated by the Wenz curves between 77 dB re 1 µPa when integrated between 20 kHz and 50 kHz for Beaufort state 3. The relatively high frequency of beaked whale signals causes them to attenuate quickly over distance, and as a result the simulations of the two array geometries (**Figures 8** and **9** for the TOA and cross-fixing arrangements, respectively) show poor localization performance. Although the biases are within 30% broadside up to a 1.5-km range, the uncertainties are higher than 60% at almost all locations. Thus, if a beaked whale signal is detected on a PAM system, one will not be able to localize it with much accuracy with a 200-m aperture array. In practice, most PAM operators conclude that if a beaked whale signal is detected, it must be within a couple of kilometers of the system, without attempting to localize.



**Figure 8.**   **Relative bias (left) and variance (right) expressed as a percentage for 20 iterations of a simulated beaked whale signal for the three-element time-of-arrival (TOA) localization geometry, incorporating 1-m uncertainty in hydrophone position**
Small black circles indicate hydrophone positions. White areas indicate locations with no valid solution.

**Figure 9.** Relative bias (left) and variance (right) expressed as a percentage for 20 iterations of a simulated beaked whale signal using the cross-fixing localization algorithm, incorporating 1-m uncertainty in hydrophone position and 10° uncertainty in subarray heading

Small black circles indicate hydrophone positions. White areas indicate locations with no valid solution.

## 3.2 Analysis of Seismic Streamer Data

The seismic streamer dataset published by Abadi et al. (2015, 2017) was used to test the algorithm described in **Section 2.3**. This dataset was recorded with a sampling rate of 500 Hz following the application of a 220-Hz low-pass anti-alias filter. A Python code capable of selecting any piece of this dataset has been prepared. **Figure 10** shows the spectrogram of three baleen whale vocalizations that have been selected for testing.

The grid search localization algorithm developed by Abadi et al. (2015, 2017) was applied to the whale vocalizations shown in **Figure 10**, and results are shown in **Figure 11**. In this figure, each subarray consists of 15 hydrophones. The solid black line shows the location of the subarrays of the streamer relative to the center of the airgun array. The gray dashed lines are the beamforming output using data recorded by each subarray. The information about the direction of arrivals limits the search area as shown in this figure. The color shading shows the travel time residual in seconds, which shows a difference between the observed and calculated travel time. The location that the travel time residual is lowest is the estimated source location which are shown with red stars. The 95% confidence levels are shown with yellow lines.
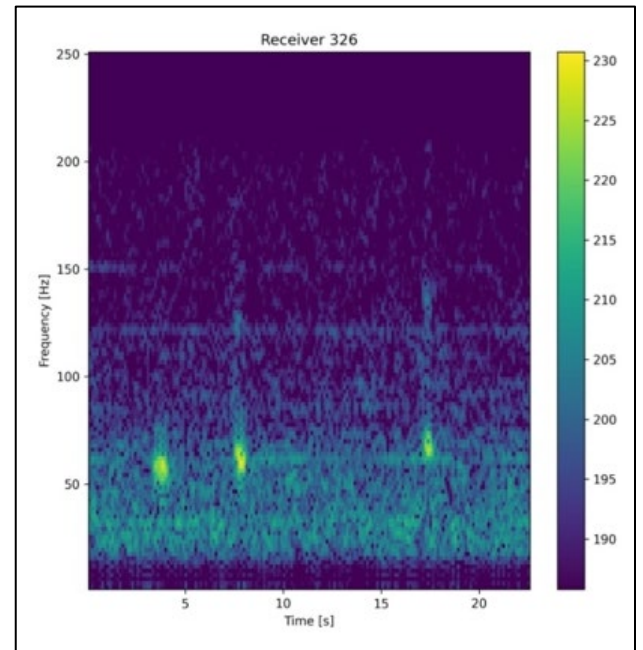


**Figure 10.** Spectrogram of three baleen whale vocalizations used for testing the algorithm developed for this project
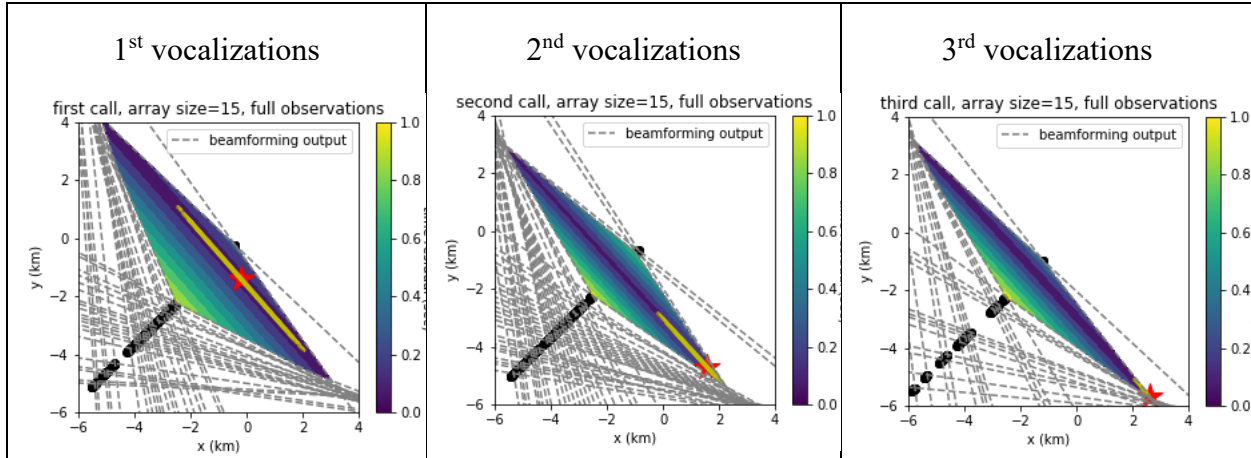
**Figure 11.  Localization result using the grid search method from Abadi et al. (2015, 2017) for a 15-element subarray for the vocalizations shown in Figure 10**

Unlike the third vocalization, the 95% confidence area is broad for the first and second vocalizations. This large uncertainty is because the algorithm assumes all three vocalizations are generated from the same area. The left/right ambiguity due to the straight streamer is noticeable in the result. This ambiguity will be eliminated if the subarrays are not arranged in a straight line.

As shown in **Figure 12**, if the number of hydrophones in the subarrays is reduced to five, the localization uncertainty (indicated by the yellow lines) increases.
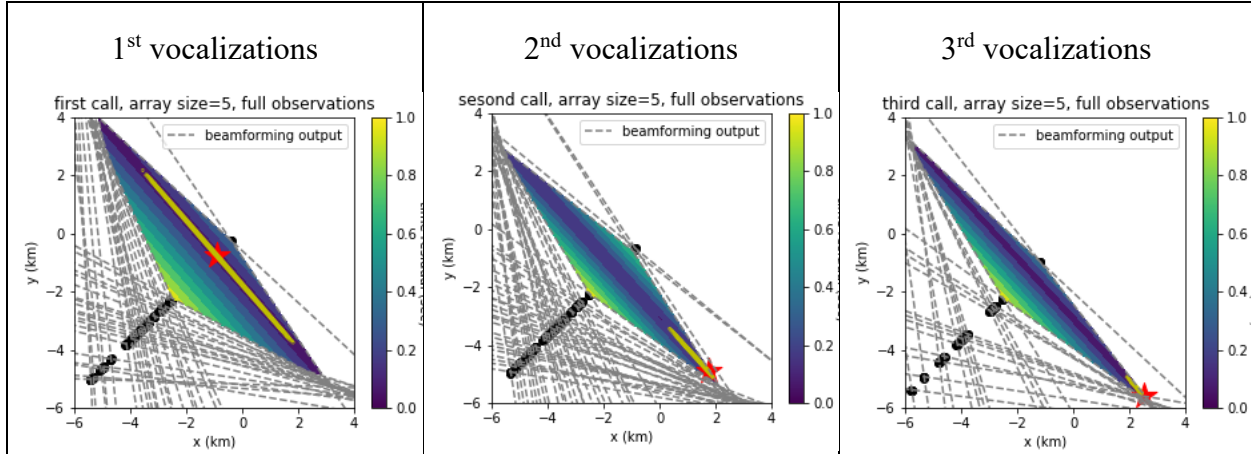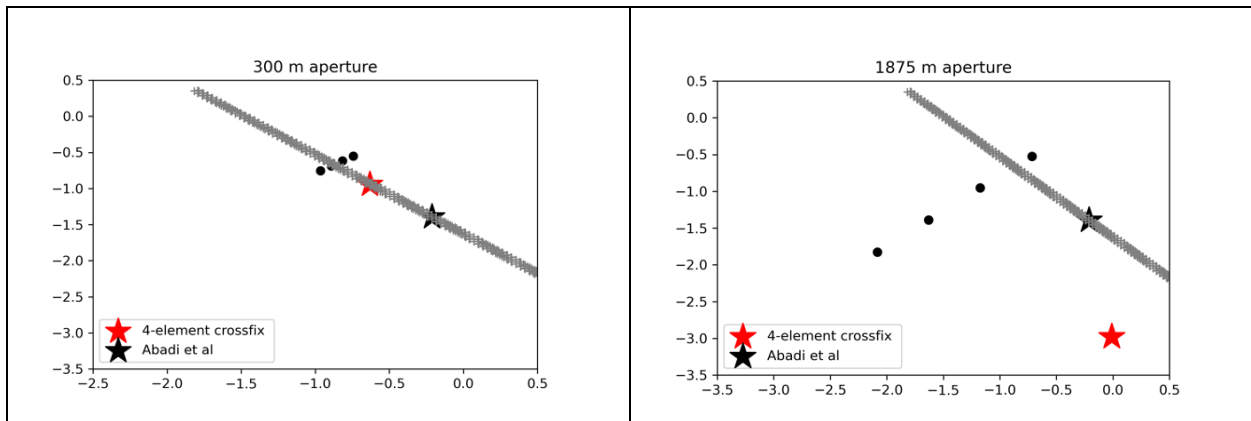


**Figure 12.  Localization result using the grid search method from Abadi et al. (2015, 2017) for a 5-element subarray for the vocalizations shown in Figure 10**

The first vocalization in **Figure 10** is used to test the two algorithms described in **Section 2.3**. The location estimated by Abadi et al. is compared with three-element TOA localization algorithm and four-element cross-fix localization algorithm in **Figure 13** and **Figure 14**, receptively. In these figures, the black circles show the location of the hydrophones relative to the center of the airgun array. The estimated location using Abadi et al. (2015, 2017) algorithm is shown with a black star. The 95% confidence levels are shown with gray plus marks. In each figure, results from a small- and large-aperture subarray are shown.

High level of background noise in the streamer recordings, vessel noise and flow noise, and uncertainty in array element positions have degraded the performance of the three-element and four-element localization algorithms. As described in **Section 2.2**, the three-element algorithm requires curved wavefronts for localization. For localizing sources far from the array, a large-aperture array is needed to achieve this curved wavefront structure. As shown in **Figure 13**, the large-aperture subarray with 1,250-m length better localize this far source. However, it is unlikely that any towed PAM array used for mitigation for offshore wind farm development will achieve that length. On the other hand, the four-element algorithm is able to estimate the azimuthal bearing correctly when the aperture is small. However, this algorithm performs worse in large-aperture array when the two hydrophones in sub-apertures are far from each other and the received signal does not have a plane wave structure.
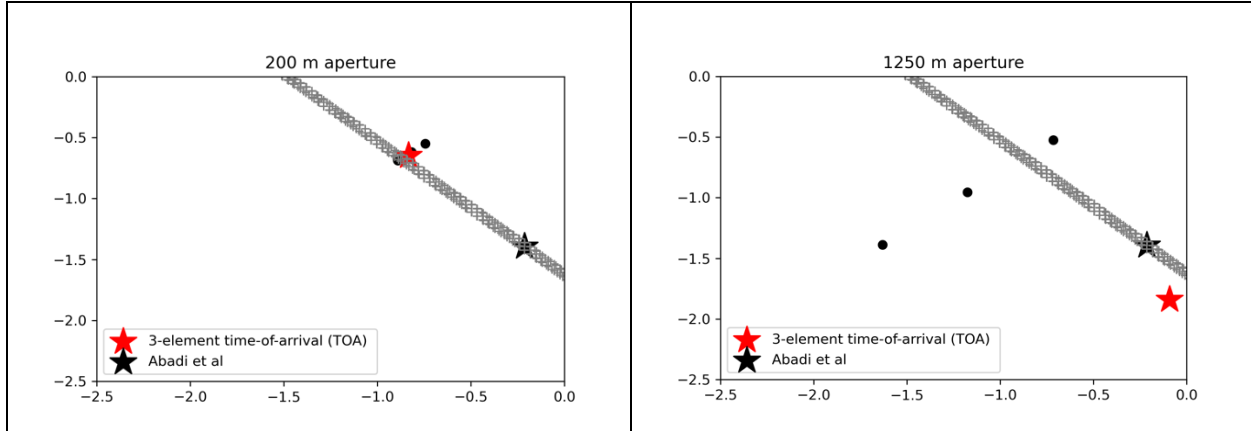


**Figure 13.** Localization result using the grid search method from Abadi et al. (2015, 2017) and three-element TOA localization algorithm for a 3-element subarray with (a) 200-m aperture and (b) 1,250-m aperture for the first vocalization shown in Figure 10.



**Figure 14.** Localization result using the grid search method from Abadi et al. (2015, 2017) and four-element cross-fix localization algorithm for a 4-element subarray with (a) 300-m aperture and (b) 1,875-m aperture for the first vocalization shown in Figure 10.

### 3.2.1   User Interface and Application

The algorithm described in **Section 2** was implemented with MATLAB software using a simple text-based user interface. A simple graphical user interface has been implemented that permits the user to manipulate a variety of text boxes, pull-down lists, and radio buttons to enter the various input parameters highlighted in *italic bold* in **Section 2.3**. Many of the interface fields have default values suggested, based

on the requirements presented in **Section 2.1**. The user interface is divided into subsections that reflect the breakdown in **Section 2.3**: array geometry, species cluster, propagation, noise, and localization method. At present, the species cluster section allows the user to select a species cluster using a drop-down menu and then generates the remaining parameters using the information in **Table 1**. The ambient noise levels can be entered directly as pairs of frequency ($f_{noise}$) and PSD (***PSD**_{noise}*), or a Beaufort Sea state (*Beaufort force* minus 1) and relative *shipping level* can also be selected to automatically generate the noise spectrum. The choice of the species cluster will also produce a default recommendation for the acoustic sampling rate.

Although MATLAB is a proprietary software, it does permit compiled versions of its applications to be created for a variety of platforms royalty-free for unlimited distribution, which will take place under the BOEM's direction and guidance.

# 4 Conclusions

A numerical model for simulating the localization performance of a three- or four-hydrophone towed PAM array on multiple species clusters was developed and documented in this report, along with some representative simulations of a 200-m aperture array for three marine mammal signal types of high interest along the U.S. eastern seaboard. The main insight from these simulations is that the uncertainty in range estimation is dominated by the uncertainty in array element positions. The reason for this is that the noise levels specified both by BOEM and the Wenz curves (from which the BOEM estimates seem to be derived) are likely too low, having been derived for measurements from a stationary platform well away from vessel noise. In consultation with BOEM, example background noise profiles from actual PAM operations will continue to be explored to determine when background noise levels become a determining factor for PAM array performance.

# 5 References

Abadi S, Tolstoy M, Wilcock W. 2015. Baleen whale localization using a dual-line towed hydrophone array during seismic reflection surveys. Journal of the Acoustical Society of America. 138(3):1762-1762.

Abadi S, Tolstoy M, Wilcock W. 2017. Estimating the location of baleen whale calls using dual streamers to support mitigation procedures in seismic reflection surveys. PLOS One. 12(2):p.e0171115.

Ainslie M, McColm J. 1998. A simplified formula for viscous and chemical absorption in sea water. Journal of the Acoustical Society of America. 103:1671-1672.

Cucknell A, Frantzis A, Boisseau O, Romagosa M, Ryan C, Tonay A, Alexiadou P, Öztürk A, Moscrop A. 2016. Harbour porpoises in the Aegean Sea, Eastern Mediterranean: the species' presence is confirmed. Marine Biodiversity. 9(1):72.

Erbe C, Dunlop R, Jenner K, Jenner M-N, McCauley R, Parnum I, Parsons M, Rogers T, Salgado-Kent C. 2017. Review of underwater and in-air sounds emitted by Australian and Antarctic marine mammals. Acoustics Australia. 45:179-241.

Hildebrand J. 2009. Anthropogenic and natural sources of ambient noise in the ocean. Marine Ecology Progress Series. 395:5-20.

Li X, Deng Z, Rauchenstein LT, Carlson T. 2016. Contributed Review: Source-localization algorithms and applications using time of arrival and time difference of arrival measurements. Review of Scientific Instruments. 87(4):041502.

Skolnik M. 1962. Introduction to Radar Systems. New York, NY: McGraw-Hill.

Spencer S. 2007. The two-dimensional source location problem for time differences of arrival at minimal element monitoring arrays. Journal of the Acoustical Society of America. 121:3579-3594.

Wenz G. 1962. Acoustic ambient noise in the ocean: spectra and sources. Journal of the Acoustical Society of America. 334:1936-1956.

**Department of the Interior (DOI)**

The Department of the Interior protects and manages the Nation's natural resources and cultural heritage; provides scientific and other information about those resources; and honors the Nation's trust responsibilities or special commitments to American Indians, Alaska Natives, and affiliated island communities.

**Bureau of Ocean Energy Management (BOEM)**

The mission of the Bureau of Ocean Energy Management is to manage development of U.S. Outer Continental Shelf energy and mineral resources in an environmentally and economically responsible way.

**BOEM Environmental Studies Program**

The mission of the Environmental Studies Program is to provide the information needed to predict, assess, and manage impacts from offshore energy and marine mineral exploration, development, and production activities on human, marine, and coastal environments. The proposal, selection, research, review, collaboration, production, and dissemination of each of BOEM's Environmental Studies follows the DOI Code of Scientific and Scholarly Conduct, in support of a culture of scientific and professional integrity, as set out in the DOI Departmental Manual (305 DM 3).